

Structure determination of the 1/1 α/β mixed lactose by X-ray powder diffraction

Jacques Lefebvre,* Jean-François Willart, Vincent Caron, Ronan Lefort, Frédéric Affouard and Florence Danède

Laboratoire de Dynamique et Structure des Matériaux Moléculaires, UMR CNRS 8024, UFR de Physique, Bâtiment P5, Université des Sciences et Technologies de Lille, 59655 Villeneuve d'Ascq CEDEX, France

Correspondence e-mail:
jacques.lefebvre@univ-lille1.fr

The mixed form of α/β lactose was obtained by heating amorphous α -lactose at 443 K. NMR spectroscopy determined the stoichiometry of this mixed compound to be 1/1. The X-ray powder diffraction pattern was recorded at room temperature with a sensitive curved detector (CPS 120). The structure was solved by real-space methods (simulated annealing) followed by Rietveld refinements with soft constraints on bond lengths and bond angles. The H atoms of the hydroxyl groups were localized by minimization of the crystalline energy. The cell of 1/1 α/β lactose is triclinic with the space group $P1$ and contains two molecules (one molecule of each anomer). The crystalline cohesion is achieved by networks of O—H \cdots O hydrogen bonds. The width of the Bragg peaks is interpreted through a microstructural approach in terms of isotropic strain effects and anisotropic size effects.

Received 14 February 2005
Accepted 30 May 2005

1. Introduction

Lactose (4-*O*- β -D-galactopyranosyl-D-glucopyranose), the milk sugar, is a carbohydrate comprising one galactose moiety linked to a glucose molecule through a β -1,4 linkage. It exhibits two anomeric forms, α -lactose and β -lactose, which differ in the configuration of the terminal hydroxyl group of the glucose unit. In the solid state, lactose can be amorphous or crystallized. Five crystalline forms are known (Garnier, 2001): α -lactose monohydrate (hereafter named α L-H₂O), hygroscopic anhydrous α -lactose (α L_H), stable anhydrous α -lactose (α L_S), β -lactose (β L) and mixed compounds of the two anomers α and β (α/β L). Four structures out of these five crystalline forms were solved: single-crystal X-ray diffraction was used for L-H₂O (Fries *et al.*, 1971; Beevers & Hansen, 1971; Noordik *et al.*, 1984) and β L (Hirotzu & Shimada, 1974). Recently we have been able to solve the structure of α L_H (Platteau *et al.*, 2004) and α L_S (Platteau *et al.*, 2005) using X-ray powder diffraction.

The mixed-lactose compounds α/β L are described in the literature with different stoichiometries; the ratio of the two anomers depends on the method used to obtain the compound. Values such as 4/1, 3/2 and 5/3 for α/β L are found in the literature (see, for example, Simpson *et al.*, 1982; Drapier-Beche, 1997). Lerk *et al.* (1984*a,b*) demonstrated the possibility of obtaining a mixed lactose with 1/1 stoichiometry by heating α L-H₂O or α L_H at 443 K.

The present paper aims to resolve the crystal structure of the mixed lactose. After the crystallization and characterization of the compound, NMR experiments were performed in order to determine its stoichiometry. The thermodynamic process used to produce the α/β L compound does not provide single crystals suitable for a four-circle diffractometer inves-

tigation. The determination of the structure was solved *ab initio* from X-ray powder diffraction using a direct-space approach (simulated annealing) and refined by Rietveld's method. Energy-minimization calculations were performed in order to locate the H-atom positions of the hydroxyl groups involved in hydrogen bonding. The width of the Bragg peaks is interpreted in terms of size and strain effects.

2. Experimental

2.1. Preliminary experiments

The crystalline α/β lactose was obtained over three steps, as described in detail by Willart *et al.* (2004):

(i) Crystalline αL_S was first produced from the dehydration of commercial crystalline $\alpha L-H_2O$ purchased from Sigma Company. Dehydration was performed by blowing dry gaseous methanol through 20 g of $\alpha L-H_2O$ for 3 h. Such a dehydration was carried out at quite low temperature (337.7 K) to prevent the formation of αL by mutarotation. The remaining traces of methanol were then removed by placing the sample under vacuum (10^{-3} mm Hg) at 293 K for 12 h.

(ii) αL was then totally amorphized at room temperature by a 23 h milling procedure performed under a dry nitrogen atmosphere in a planetary mill (Pulverisette 7/Fritsch).

(iii) Amorphous αL_S was then heated up to 443 K at 2 K min^{-1} , kept at this temperature for 10 min and then cooled down to room temperature. This thermal treatment has been shown previously (Willart *et al.*, 2004) to induce both a strong mutarotation process and the complete crystallization of amorphous αL towards the mixed compound $\alpha/\beta L$.

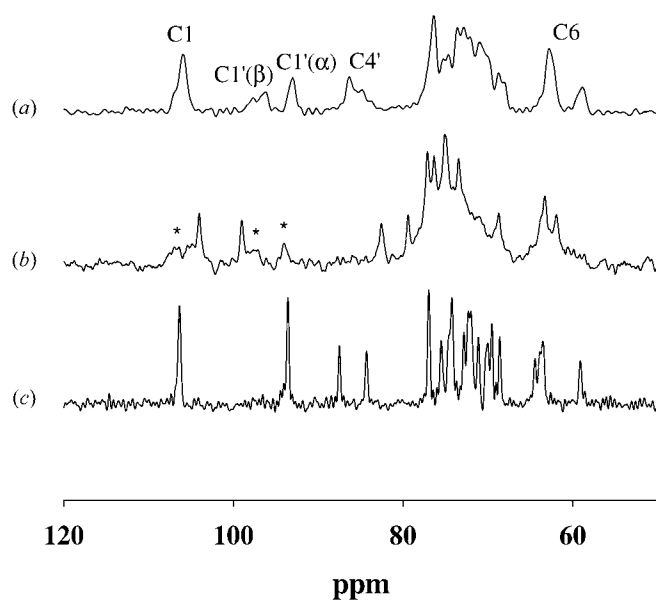


Figure 1
 ^{13}C CPMAS spectrum of (a) mixed lactose, (b) β -lactose and (c) anhydrous stable α -lactose. The lines marked by asterisks are assigned to the residual amorphous lactose.

NMR measurements were used to determine the stoichiometry of this mixed form. ^{13}C CPMAS NMR experiments were carried out at 100.6 MHz on a Bruker AV400 solid-state NMR spectrometer. ^1H liquid-state experiments were also performed at 400.33 MHz on a Bruker ASX400 NMR spectrometer. In this case, a powder of mixed lactose was dissolved in dimethyl sulfoxide in order to hinder the mutarotation (Dincer *et al.*, 1999). Fig. 1 displays the ^{13}C CPMAS spectrum of the mixed lactose in comparison to those of the crystalline αL_S and αL forms. The two NMR lines observed at 93.0 and 96.2 p.p.m. are assigned to the resonance of the glucose C1' anomeric C atom, respectively, in conformations α and β . Integration of the area of these two lines yields an α/β ratio of 1/1, in agreement with a parallel quantification made by ^1H liquid-state NMR. On the other hand, systematic chemical shift differences were observed in all regions of the three spectra and were especially remarkable for the primary alcohol C6 (55–65 p.p.m.) and for the glucose C4' atoms (81–90 p.p.m.). This demonstrates that the α/β compound is not a mixture of two crystalline forms of the α -lactose and β -lactose anomers, but a new crystalline form containing the two anomers.

2.2. Data collection and structure solution

The X-ray powder diffraction pattern was recorded on a laboratory diffractometer equipped with an INEL curved sensitive detector (CPS120). A bent quartz monochromator allowed the selection of the $K\alpha_1$ wavelength of a Cu X-ray tube ($\lambda = 1.54056\text{ \AA}$). The powder was introduced into a Lindemann glass capillary (diameter = 0.7 mm), and mounted on the axis of the diffractometer. The capillary was rotated during the experiment in order to reduce the effect of a possible preferred orientation. Calibration of the curved detector was performed with an X-ray diffraction pattern of the standard compound $\text{Na}_2\text{Ca}_3\text{Al}_2\text{F}_{14}$ (NAC; Evain *et al.*, 1993). A cubic spline interpolation was performed between the peaks of NAC. The curved detector has 4096 channels; the 2θ range recorded was $0.3\text{--}114.7^\circ$ and the step between two channels was 0.029° . The pattern of NAC was also used to determine the shape and parameters of the instrumental resolution; it is a pseudo-Voigt function, with the Caglioti function for the θ dependence of the Gaussian component (Caglioti *et al.*, 1958). The parameters are: $U_{\text{ins}} = 0.0186$ (4), $V_{\text{ins}} = -0.0195$ (6) and $W_{\text{ins}} = 0.0121$ (2) deg^2 . The θ dependence of the Lorentzian component is such that

$$\Gamma_L = X_{\text{ins}} \tan \theta + (Y_{\text{ins}} / \cos \theta),$$

with $X_{\text{ins}} = 0.0181$ (16) $^\circ$ and $Y_{\text{ins}} = 0.0188$ (7) $^\circ$. Data were collected at room temperature with a total counting time of 16 h 40 min.

The X-ray pattern exhibits Bragg peaks different to those of the four α - and β -lactose forms. In particular, a peak appears at $2\theta = 18.2^\circ$ which is, according to Buma & Wiegers (1967), characteristic of the mixed $\alpha/\beta L$ form. The intensity of the peaks decreases rapidly when the Bragg angle increases. This

behaviour is generally the consequence of a disorder of the molecules in the cell.

To determine the lattice parameters, the profiles and positions of the 50 reflections with a 2θ angle lower than 41° were individually refined with the program *WinPlotr* (Roissel & Rodriguez-Carvajal, 2002*a,b*); 22 of them ranging from 4.5 to 28.5° were introduced into the program *TREOR* (Werner *et al.*, 1985) and a triclinic cell indexed these reflections. The calculated lattice parameters are: $a = 7.621$, $b = 19.680$, $c = 5.062$ Å, $\alpha = 95.6$, $\beta = 105.6$, $\gamma = 81.0^\circ$, $V = 720.9$ Å³; the values of the figures of merit are: $M(22) = 17$, $F(22) = 41$ (0.010, 55; de Wolff, 1968; Smith & Snyder, 1979). The volume of this cell is similar to the volumes of the two anhydrous forms of α -lactose and β L [730.3 Å³ for α L_H (Platteau *et al.*, 2004), 720.2 Å³ for α L_S (Platteau *et al.*, 2005) and 716.7 Å³ for β L (Hirotzu & Shimada, 1974)]; therefore, these cells have the same number of molecules, $Z = 2$. For the mixed 1/1 α/β L, the unit cell contains one molecule of α -lactose and one molecule of β -lactose. The only possible space group is *P1*.

To confirm the cell found by *TREOR*, refinements were carried out with the 'profile matching' option (Le Bail *et al.*, 1988; profile refinement) of the program *FULLPROF* (Rodriguez-Carvajal, 2001). In order to obtain a starting structural model, parameters calculated with this program were used as input parameters for the Monte-Carlo simulated annealing program (*FOX*; Favre-Nicolin & Cerny, 2002). The section of the X-ray pattern used for these refinements ran from 7 to 56° , 2θ . The lower limit, 7° , allows the inclusion of the first well defined reflection; there were enough reflections between 7 and 56° for the use of *FOX*. The profile of the reflections was fitted with a pseudo-Voigt function with the same FWHM for the Gaussian and the Lorentzian components. This FWHM has a θ dependence according to Caglioti's law (Caglioti *et al.*, 1958) and the Lorentzian contribution to the pseudo-Voigt function is a linear function of 2θ . The asymmetry of the peaks was taken into account according to Bérar & Baldinozzi's (1993) function. The background was determined with a linear interpolation between 19 points regularly distributed between 7 and 56° . At the end of the 'profile matching' refinements, the conventional agreement factors are: $R_p = 0.0583$, $R_{wp} = 0.0600$, $R_{exp} = 0.0220$ and $\chi^2 = 7.43$. These values confirm the validity of the cell found by *TREOR*. The lattice parameters of the 1/1 α/β L phase are: $a = 7.6231$ (7), $b = 19.650$ (2), $c = 5.0606$ (6) Å, $\alpha = 95.646$ (3), $\beta = 105.392$ (3), $\gamma = 80.977$ (3)°, $V = 720.54$ (13) Å³.

The 'parallel tempering' algorithm of the program *FOX* (Favre-Nicolin & Cerny, 2002) was used in order to obtain a starting structural model. Lattice and profile parameters, zero-point and interpolated backgrounds which were previously calculated were introduced into this program for a 2θ range running from 7 to 50° . Molecules with only C and O atoms were modelled with bond lengths, bond angles and torsion angles calculated from the atomic coordinates of Fries *et al.* (1971) for α -lactose and Hirotzu & Shimada (1974) for β -lactose. These two molecules were introduced randomly into the cell with the space group *P1*. During the simulated-annealing procedure, the bond lengths and angles were kept

constant and the rings of the galactose and glucose units were rigid. The torsion angles of the central linkage and those positioning the peripheral C and O atoms could change, leading to 37 degrees of freedom: three rotations of the whole molecule, four torsion angles for the central linkage and ten for the peripheral atoms for each molecule and three translations of the whole molecule for one of them. Torsion angles defining the position of the peripheral atoms can change during the simulated annealing procedure because significant differences were observed for the molecules of the four known structures of lactose. The integrated wR factor was 0.059 after *ca* 20 million trials. The atomic coordinates found at the end of this calculation provide an acceptable starting solution because the lowest contact distance between non-H atoms of neighbouring molecules equals 2.02 Å.

2.3. Rietveld refinements

Atomic coordinates of C and O atoms obtained with *FOX* are introduced into the program *FULLPROF* (Rodriguez-Carvajal, 2001) to perform Rietveld refinements.

To locate H atoms, two different strategies were used for CH and CH₂ groups, on the one hand, and for OH groups on the other. As each C atom was at the centre of a tetrahedron, the H atoms of the CH and CH₂ groups were positioned so that they complete the tetrahedron. For the CH groups, the three C—C—H or O—C—H bond angles were equal and the value of the C—H bond length was 1.00 Å. For the CH₂ groups, the H—C—H angle was 107° , the H/C/H plane was perpendicular to the C/C/O plane with the two H atoms symmetrically located with respect to the previous plane. These calculations were performed with the program *DEBVIN* (Brückner & Immirzi, 1997).

The positions of the H atoms of the OH groups involved in hydrogen bonds were determined by crystalline energy minimization with the DL_POLY molecular modelling package (Smith & Forester, 1996) on a system of $N = 80$ ($4 \times 2 \times 5$ crystalline cells) lactose molecules using periodic boundary conditions. Each molecule was described by its 45 atoms which interact through the Ha force field (Ha *et al.*, 1988). This method corresponded to the case of carbohydrates and electrostatic interactions were handled by Ewald's method. A cut-off radius of 10 Å was used. Energy minimization calculations were carried out from the structure obtained experimentally. In order to maintain the experimental structure as much as possible, only H atoms of the hydroxyl groups are allowed to move.

During the Rietveld refinements, the position of the H atom was shifted according to the C or O atom to which it was bonded. Owing to the possibility of the deformation or rotation of the molecules, the positions of the H atoms were recalculated three times during the refinement procedure either with *DEBVIN* or by energy minimization.

Owing to the rapid decrease of X-ray intensity with Bragg angle, the 2θ range for the Rietveld refinements runs from 7 to 70° . The reduced coordinates of the central O11 atom were fixed and those of the other 45 non-H atoms were adjusted.

Table 1

Bond lengths (Å) and angles (°) for the soft constraints.

The mean values and their root mean-square deviations were obtained after Rietveld refinements. The subscript 'int' represents the internal atoms of the cycles; 'per' represents the peripheral atoms. The C and O atoms of the methanol groups are named C_m and O_m , and O_{link} is the O atom linking the two units.

	Constraint values	Calculated mean values
$C_{int}-C_{int}$	1.527	1.531 (17)
$C_{int}-O_{int}$	1.433	1.433 (16)
$C_{int}-C_m$	1.511	1.510 (18)
$C_{int}-O_{per}, C_m-O_m$	1.421	1.421 (17)
$C_{int}-O_{link}$	1.421	1.426 (8)
$C_{int}-C_{int}-C_{int}$	110.4	109.9 (29)
$C_{int}-C_{int}-O_{int}$	109.6	109.7 (30)
$C_{int}-O_{int}-C_{int}$	113.2	113.6 (11)
$C_{int}-C_{int}-C_m$	112.8	115.3 (49)
$O_{int}-C_{int}-C_m$	107.1	107.4 (44)
$C_{int}-C_{int}-O_{per}$	110.4	110.0 (42)
$C_{int}-C_m-O_m$	108.4	106.8 (40)
$O_{int}-C_{int}-O_{per}$	109.5	107.9 (23)
$C_{int}-C_{int}-O_{link}, O_{int}-C_{int}-O_{link}$	107.9	109.2 (47)
$C_{int}-O_{link}-C_{int}$	116.8	117.8 (25)

The root mean-square deviation σ is defined as: $\sigma = \{[\sum_{i=1}^N (V_i - V_{mean})^2]/N\}^{1/2}$, where N is the number of observations.

Taking into account the large number of free parameters with respect to the number of Bragg peaks with a significant intensity, soft restraints were introduced on all bond lengths and angles. The restraint values were taken to be the mean values found in some disaccharides with a β -1,4 linkage and with structures solved from single crystals (β -cellobiose: Chu & Jeffrey, 1968; methyl β -cellobioside: Ham & Williams, 1970; α -lactose monohydrate: Fries *et al.*, 1971; β -lactose: Hirotsu & Shimada, 1974). These values are listed Table 1 for the

different combinations of atoms involved in the lactose molecule. With such restraints in bond lengths and angles, only the torsion angles are completely free. To define the conformations of the non-H atoms of a lactose molecule, only 20 torsion angles are necessary. For each of the two molecules, the atoms of a given unit had a common isotropic displacement parameter. Intensities were corrected for absorption effects of a cylindrical sample with a μR value of 0.40.

A pseudo-Voigt profile function with the Thompson–Cox–Hastings formalism (Thompson *et al.*, 1987) was used to fit the peaks of the X-ray pattern. This function takes into account the instrument resolution, and size and strain effects. These two effects can affect broadening of the peaks in an isotropic or anisotropic way. The angular dependencies of the FWHM of the Gaussian (H_{Gf}) and Lorentzian (H_{Lf}) components are given by Rodriguez-Carvajal & Roisnel (2004). Le Bail refinements were performed with the four possibilities of isotropy and anisotropy; Rietveld agreement factors are reported in Table 2. The best R_{wp} value is obtained when the two effects are anisotropic, but in this case some Gaussian widths are negative and this solution should be excluded. The model chosen combined isotropic strain effects and anisotropic size effects to obtain the best R_{wp} improvement, while keeping physically sensible parameter values. Anisotropic size broadening was introduced by spherical harmonics functions, $Y_{l,m}$ (Popa, 2000).

The March (1932) and Dollase (1986) function was used to account for the preferred orientation. After several attempts, the best R_{wp} value was obtained when the preferred orientation was along [100] and as this effect was small, only the parameter G_1 was fitted.

For the final Rietveld refinements, there were 182 fitted parameters:

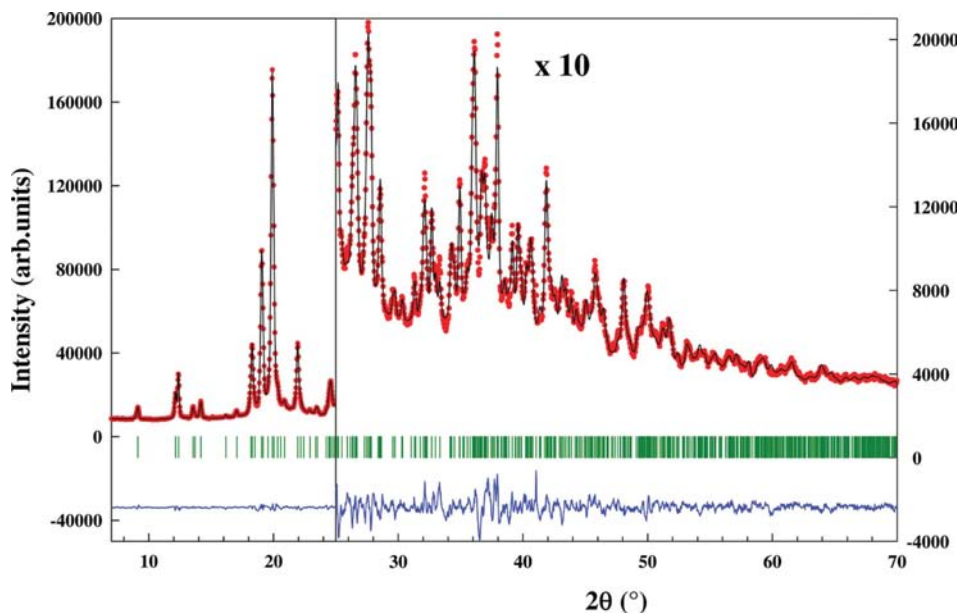


Figure 2

Final Rietveld plot of the mixed phase of α/β -lactose. Observed data points are indicated by dots, the best-fit profile (upper trace) and the difference pattern (lower trace) are shown as solid lines. The vertical bars correspond to the positions of the Bragg peaks.

(i) 17 profile parameters: the zero-point parameter, six lattice parameters, U_{ST} , G_{SZ} , six parameters for the anisotropic size effects and the two first parameters of the Bérar & Baldinozzi (1993) function for the asymmetry of the peaks.

(ii) 141 structural parameters: the scale factor, 135 adjustable coordinates for the 45 non-H atoms (the coordinates of O11 were fixed), four isotropic displacement parameters and a parameter (G_1) linked to the preferred orientation according to the March (1932) and Dollase (1986) function. The number of adjustable coordinates is, in fact, reduced by the introduction of 48 soft restraints on bond lengths and 70 on bond angles.

(iii) The value of 24 points regularly distributed between 7 and 70°, 2θ , to define the background.

Table 2

Profile agreement factors and average apparent values when size and strain effects are taken to be either isotropic or anisotropic.

For the isotropic effect, the standard uncertainties are given in parentheses. When the effect is anisotropic, the number in parenthesis is the dispersion with respect to the average value.

	Isotropic size Isotropic strain	Anisotropic size Isotropic strain	Isotropic size Anisotropic strain	Anisotropic size Anisotropic strain
R_p	0.0546	0.0478	0.0497	0.0459
R_{wp}	0.0593	0.0486	0.0525	0.0460
R_{exp}	0.0213	0.0213	0.0212	0.0212
χ^2	7.78	5.22	6.14	4.73
Average size (Å)	531 (1)	549 (100)	553 (1)	525 (106)
Average strain ($\times 10^{-4}$)	17.62 (1)	17.68 (5)	21.40 (912)	18.32 (727)

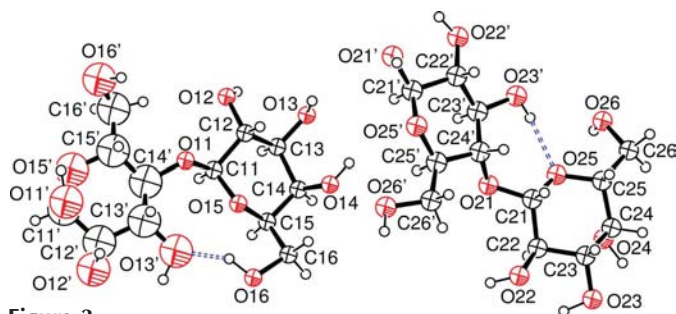
The final conventional Rietveld factors are: $R_p = 0.0747$, $R_{wp} = 0.0791$, $R_{exp} = 0.0229$ and $\chi^2 = 11.9$, $R_B = 0.0304$ and $R_F = 0.0372$. The root mean-square deviations from the soft restraints are 0.017 \AA for the bond lengths and 3.9° for the bond angles. The mean value of the electronic density synthesis is zero with a root mean-square deviation of 0.05 e \AA^{-3} ; the values of the highest peak and the deepest hole being equal to 0.019 and $-0.019 \text{ e \AA}^{-3}$, respectively. A plot of the X-ray pattern is given in Fig. 2. A view of the two molecules of lactose, drawn with ORTEP3 (Farrugia, 1997) and showing the atomic numbering scheme, is presented in Fig. 3. Crystallographic data, and profile and structural parameters, are reported in Tables 3 and 4, respectively.¹ The molecular packing in the ab plane is drawn in Fig. 4.

3. Discussion

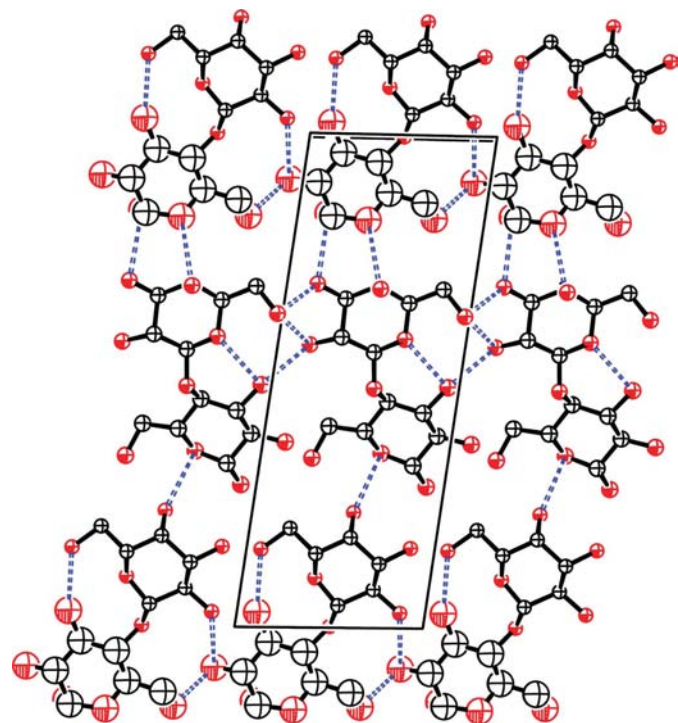
Table 1 gives the mean values with their r.m.s. deviations for the different types of bond lengths and angles. The mean bond lengths are close to those of the soft restraints. For most types of bond length, significant root mean-square deviations are observed which are at least twice the values obtained for αL_H (Platteau *et al.*, 2004) and αL_S (Platteau *et al.*, 2005). The highest discrepancy between calculated and soft restraint values is observed for $C24' - C25'$, where the difference equals 0.038 \AA . For the β -1,4 linkage, the bond lengths on both sides of the central O atom are very similar with a difference of 0.005 \AA for the first molecule and 0.014 \AA for the second molecule. The mean bond angles are also close to the restraints values, except for $C_{int} - C_{int} - C_m$, where the difference reaches 2.5° . Nevertheless, some calculated angles differ up to 11° from the restraint values, which is the case in particular for angles where the central $Oi1$ atoms are involved.

For the two molecules of the unit cell, identification with the anomers must be obtained from typical torsion angles. The main difference between α - and β -lactose molecules involves the position of the terminal $Oi1'$ atom of the glucose unit: it is the mutarotation which allows the α -lactose anomer to

transform into the β -lactose. The torsion angles around the central linkage also differ for the two anomers. Table 5 reports, for the five crystalline forms of lactose, the torsion angles around the β -1,4 linkage and those where the $Oi1'$ atoms are involved. For the molecule of α -lactose, a symmetric twist about the bridging bonds is formed, leading to the following equalities between the torsion angles: $|\psi_1| \simeq |\psi_2|$ and $|\psi_1'| \simeq |\psi_2'|$. For β -lactose, the twist is asymmetric and the differences

**Figure 3**

Atomic numbering and structure of the molecules of α - and β -lactose. The notation of atoms Xin is such that $X = C, O$; $i = 1, 2$ for molecules α - and β -lactose, respectively; n is the number of the atom; unprimed atoms correspond to the galactose unit, primed atoms to the glucose unit. Dashed lines correspond to intramolecular hydrogen bonds.

**Figure 4**

Projection along c^* of the unit cell of the mixed phase of α/β -lactose. Dashed lines correspond to hydrogen bonds (the horizontal axis is a).

¹ Supplementary data for this paper are available from the IUCr electronic archives (Reference: LC5025). Services for accessing these data are described at the back of the journal.

Table 3

Crystallographic data for the mixed phase of α/β -lactose obtained after Rietveld refinements.

Formula	C ₁₂ H ₂₂ O ₁₁
<i>M_r</i>	342.30
Crystal system	Triclinic
Space group	<i>P</i> 1
<i>a</i> (Å)	7.6258 (4)
<i>b</i> (Å)	19.6559 (10)
<i>c</i> (Å)	5.0613 (3)
α (°)	95.646 (2)
β (°)	105.430 (2)
γ (°)	80.996 (2)
<i>V</i> (Å ³)	721.00 (7)
<i>Z</i>	2
<i>D_c</i> (g cm ⁻³)	1.576
<i>F</i> (000)	364
μ (mm ⁻¹)	1.23
2 θ range (°)	7–70
Step size (° 2 θ)	0.029
Wavelength (Å)	1.54056
No. of profile data steps	2172
No. of contributing reflections	621
No. of structural variables	141
No. of profile parameters	17
No. of background points refined	24
No. of bond length constraints	48
No. of bond angle constraints	70
<i>R_p</i>	0.0748
<i>R_{wp}</i>	0.0791
<i>R_e</i> ^{exp}	0.0229
χ^2	11.9
<i>R_B</i>	0.0304
<i>R_F</i>	0.0372

between $|\psi_1|$ and $|\psi_2|$, on one hand, and $|\psi'_1|$ and $|\psi'_2|$, on the other hand, reach 40°. In the present case, $|\psi_1| \simeq |\psi_2|$ and $|\psi'_1| - |\psi'_2| = 14.0^\circ$ for the first molecule, and $|\psi_2| - |\psi_1| = 11.0^\circ$ and $|\psi'_1| - |\psi'_2| = 3.9^\circ$ for the second molecule. The conformation of the two molecules of the present form is an intermediate case between the two anomers, as found in methyl β -cellobioside (Ham & Williams, 1970). For the torsion angles with Oi1' as the terminal atom, from the four crystalline forms of lactose where the structure is known, the following values were found: $\psi_3 \simeq -60^\circ$, $\psi'_3 \simeq \psi_4 \simeq 60^\circ$ for a β -lactose molecule and $\psi_3 \simeq \psi_4 \simeq 180^\circ$ and $\psi'_3 \simeq -60^\circ$ for β -lactose. With the values reported in Table 5 for α/β L, the first molecule is, unambiguously, the α -anomer and the second one is the β -anomer.

For each of the two molecules of the unit cell, different global isotropic displacement parameters were introduced for the two units which led to a significant improvement in the Rietveld agreement factor *R_{wp}*. These calculated parameters are approximately equal for the second molecule [the two values 3.0 (4) and 3.3 (3) Å² are in the error bars]. They are significantly different for the first molecule with a value of 2.4 (3) Å² for the galactose unit and 8.7 (5) Å² for the glucose unit. This high value is probably a consequence of an orientational disorder of this unit, as expected from the rapid decrease of the X-ray intensity when the Bragg angle increases. Nevertheless, with a triclinic symmetry it is impossible to characterize this disorder.

The lattice parameters of the five crystalline forms of lactose are reported in Table 6. Apart from β L, the parameters of the four other cells agreed closely with the average values

Table 4

Profile and structural parameters for the mixed phase of α/β -lactose obtained by *FULLPROF* (Rodriguez-Carvajal, 2001) after Rietveld refinements.

An explanation of the symbols used in this table is given by Rodriguez-Carvajal & Roisnel (2004).

<i>U_{ST}</i>	0.228 (13)
<i>G_{SZ}</i>	-0.0026 (4)
<i>C₀₀</i>	1.54 (4)
<i>C₂₀</i>	0.10 (4)
<i>C₂₁₊</i>	0.13 (4)
<i>C₂₁₋</i>	-0.48 (5)
<i>C₂₂₊</i>	-0.51 (4)
<i>C₂₂₋</i>	0.25 (5)
Asym ₁	0.021 (9)
Asym ₂	0.0048 (7)
Preferred orientations	[1, 0, 0]
<i>G₁</i>	0.953 (5)
<i>B_{iso}</i> first mol. galactose (Å ²)	2.4 (3)
<i>B_{iso}</i> first mol. glucose (Å ²)	8.7 (5)
<i>B_{iso}</i> second mol. galactose (Å ²)	3.0 (4)
<i>B_{iso}</i> second mol. glucose (Å ²)	3.3 (3)

of *a* and *c* of 7.76 and 4.94 Å, respectively. For the three anhydrous forms, the average *b* parameter was 19.74 Å. The presence of a water molecule in α L-H₂O increased this parameter to 21.562 Å. The β angle ranges from 103.7 to 109.6° and the α angles for the two triclinic cells were close to 90°. Finally, the most significant change was observed with the γ angle of α L_H and α/β L, with a difference of 7 and 9° with respect to the two monoclinic forms of the α -anomer. As a consequence, for these four forms with similar cells, the long axis of the molecule of lactose was along *b* with the following sequence when the *y* coordinate increased: glucose, then galactose units of the first molecule and then two units in the same order for the second molecule. For the α/β L form, the *ac* plane at *y* \simeq 0.0 contains α -lactose molecules and the β -lactose molecules are in the same plane at *y* \simeq 0.5.

For carbohydrates, the cohesion lattice energy is mostly provided by O—H...O hydrogen bonds. A crystalline energy minimization was performed in order to locate the H atoms of the hydroxyl groups and, consequently, to define the hydrogen-bonding geometry. The hydrogen-bonding distances and angles obtained with these calculations are listed Table 7 and Fig. 4 shows the hydrogen-bonding networks in the *ab* plane. Geometric arguments, as explained in a previous article (Platteau *et al.*, 2005), were also used to check the calculations. Finally, the O atoms of the 16 hydroxyl groups are donors; O11, O13, O15, O11', O16', O21, O24 and O21' are not acceptors, O12 and O13' are double acceptors, and the 12 other O atoms are single acceptors. It is noteworthy that among the eight non-acceptor O atoms of the present form, six of them are also non-acceptors in α L_S (Platteau *et al.*, 2005) and five in α L_H. The O...O distances range from 2.48 to 3.09 Å with an average value of 2.78 Å (value found in carbohydrates; Jeffrey, 1990), but with a large root mean-square deviation of 0.20 Å. Unlike α L_H and α L_S, the energy minimization leads to incorrect positions for some H atoms. For HO11, HO13' and HO21' the H...O distances are higher than 2.7 Å and the O—H...O angles are smaller than 100°.



Table 5

Torsion angles ($^{\circ}$) of the different crystalline forms of lactose.

(a) Around the α -1,4 linkage. ψ_1 , ψ_1' , ψ_2 and ψ_2' are defined according to Sundaralingam (1968): $\psi_1 \equiv \text{O5}-\text{C1}-\text{O1}-\text{C4}'$, $\psi_1' \equiv \text{C2}-\text{C1}-\text{O1}-\text{C4}'$, $\psi_2 \equiv \text{C1}-\text{O1}-\text{C4}'-\text{C3}'$, $\psi_2' \equiv \text{C1}-\text{O1}-\text{C4}'-\text{C5}'$.

		ψ_1	ψ_1'	ψ_2	ψ_2'
$\alpha/\beta\text{L}^a$	First molecule	-90.4 (10)	159.1 (8)	96.6 (10)	-145.0 (8)
	Second molecule	-91.1 (17)	141.0 (13)	102.1 (15)	-137.1 (14)
αL_S^b	First molecule	-85.9 (13)	155.6 (11)	69.2 (14)	-160.9 (10)
	Second molecule	-87.3 (10)	148.8 (8)	87.0 (10)	-153.0 (7)
αL_H^c		-92.3 (11)	148.1 (9)	91.5 (11)	-150.9 (9)
$\alpha\text{L}-\text{H}_2\text{O}^d$		-92.6	146.2	94.6	-143.0
βL^e		-70.7	170.3	108.0	-131.3

(b) Characterizing the α -lactose and β -lactose anomers. $\psi_3 \equiv \text{O1}'-\text{C1}'-\text{C2}'-\text{C3}'$; $\psi_3' \equiv \text{O1}'-\text{C1}'-\text{C2}'-\text{O2}'$; $\psi_4 \equiv \text{O1}'-\text{C1}'-\text{O5}'-\text{C5}'$.

		ψ_3	ψ_3'	ψ_4
$\alpha/\beta\text{L}^a$	First molecule	-76.0 (15)	41.5 (16)	60.7 (21)
	Second molecule	179.7 (12)	-54.1 (17)	-178.5 (14)
αL_S^b	First molecule	-81.1 (12)	55.3 (12)	60.6 (14)
	Second molecule	-60.4 (12)	63.3 (12)	59.6 (13)
αL_H^c		-71.5 (12)	57.1 (14)	72.2 (12)
$\alpha\text{L}-\text{H}_2\text{O}^d$		-68.4	57.8	59.0
αL^e		177.1	-66.6	176.3

References: (a) this paper; (b) Platteau *et al.* (2005); (c) Platteau *et al.* (2004); (d) Fries *et al.* (1971); (e) Hirotsu & Shimada (1974).

Table 6

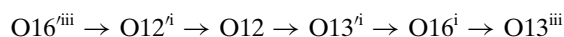
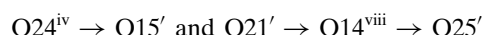
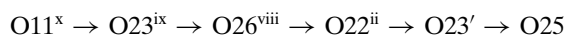
Space group and lattice parameters of the different crystalline forms of lactose.

	$\alpha/\beta\text{L}^a$	αL_S^b	αL_H^c	$\alpha\text{L}-\text{H}_2\text{O}^d$	βL^e
Space group	$P1$	$P1$	$P2_1$	$P2_1$	$P2_1$
a (\AA)	7.6258 (4)	7.6522 (2)	7.7795 (3)	7.982 (2)	10.839 (6)
b (\AA)	19.6559 (10)	19.8637 (5)	19.6931 (7)	21.562 (3)	13.349 (6)
c (\AA)	5.0613 (3)	4.9877 (1)	4.9064 (1)	4.824 (1)	4.954 (5)
α ($^{\circ}$)	95.646 (2)	92.028 (1)	90	90	90
β ($^{\circ}$)	105.430 (2)	106.261 (1)	103.691 (2)	109.57 (3)	91.31 (9)
γ ($^{\circ}$)	80.996 (2)	97.153 (1)	90	90	90
V (\AA^3)	721.00 (7)	720.18 (3)	730.32 (4)	782.3 (5)	716.7 (15)

References: (a) this paper; (b) Platteau *et al.* (2005); (c) Platteau *et al.* (2004); (d) Fries *et al.* (1971); (e) Hirotsu & Shimada (1974).

The problem for the location of the H atoms of the hydroxyl groups could be a consequence of orientational disorder.

O15', O25 and O25', which are acceptors only, are at the end of the hydrogen-bonding finite chains. The five non-acceptor O atoms belonging to an hydroxyl group, O13, O11', O16', O24 and O21', are at the beginning of a finite chain. In fact, there are only four finite chains (see symmetry code at the bottom of Table 7).



The last chain has two ends, and O12 and O13', which are twice acceptors, are also donor and acceptor between themselves. Finally, there is one infinite chain as shown below.

The most original feature concerning the hydrogen-bond networks is the lack of internal O13'—HO13'...O15 hydrogen bonds which exist for all the lactose molecules of the four other crystalline forms. This hydrogen bond plays a major role in the stability of the molecule. Its absence can explain an orientational disorder of the glucose unit of the α -lactose molecule. Apart from this change, the hydrogen-bond networks of the αL_S form and the present form are alike. The two first finite chains and the infinite chain are common to the two forms. The first finite chain connects α -lactose molecules in the same *ac* plane and the second chain makes the cohesion between the β -lactose molecule located at $y \simeq -0.5$ and the α -lactose molecule at $y \simeq 0.0$. The infinite chain allows interactions between β -lactose molecules in the same *ac* plane.

For the third finite chain, in the $\alpha/\beta\text{L}$ form, only the O21'—HO21'...O14^{viii} hydrogen bond is added with respect to the αL_S form and it is a consequence of the mutarotation of O21'. This chain connects the α - and β -lactose molecules of the unit cell. The fourth chain is, in fact, a combination of two chains of αL_S . In this form, a finite chain is: O16' \rightarrow O12' \rightarrow O12 \rightarrow O13' \rightarrow O15; as there is no O13'—HO13'...O15 internal hydrogen bond, HO13' therefore interacts with the O12 atom of a neighbouring molecule. The second infinite chain of αL_S is: \rightarrow O13 \rightarrow O16 \rightarrow O13 \rightarrow with O21' linked to O13. In $\alpha/\beta\text{L}$, with the mutarotation of O21', this atom now interacts with O24. As a consequence, the position of O13 changes, the O16 \rightarrow O13 hydrogen bond disappears and a new O16—HO16...O13' internal hydrogen bond is formed. O13 \rightarrow O16 is now tied to O13'.

The direction of the preferred orientation is found along [100] with G_1 equal to 0.953 (5) and G_2 fixed at 0. This value of G_1 corresponds to a needle-like habit of the crystallites along [100].

From the powder diffraction we can deduce, from the shape and the width of the Bragg peaks, the size of the crystallites and the strain of the cell. For this study, the final Rietveld refinements were performed with isotropic strain effects and anisotropic size effects. The average value of the strain of the unit cell equals $22.20(4) \times 10^{-4}$. This value is quite large because of the presence of many defects, which is generally the case when the powder has been heated. The average calculated diameter of the crystallites equals 563 \AA with a root mean-square deviation of 106 \AA . The extreme values of the diameter of the crystallites are 390 \AA along $[-1, -6, 1]$ and 806 \AA in the $[-4, 3, 1]$ direction. Fig. 5 shows different sections of the average shape of the crystallites in the (**b**, **c***, **b**^**c***) orthogonal system. Taking into account the values close to 90° for the angles α and γ , the **b**^**c*** direction is close to **a***. The crystallites have a stick shape with the long axis approximately

Table 7
Hydrogen-bonding geometry (Å, °) for the mixed phase of α/β -lactose.

$D-H \cdots A$	$D-H$	$H \cdots A$	$D \cdots A$	$D-H \cdots A$
O12—HO12 \cdots O13 ⁱ	0.983	1.92 (4)	2.86 (4)	159.9 (16)
O13—HO13 \cdots O16 ⁱⁱ	0.988	2.07 (3)	2.96 (4)	148.5 (21)
O14—HO14 \cdots O25 ⁱⁱⁱ	0.972	1.99 (3)	2.60 (3)	118.5 (19)
O16—HO16 \cdots O13 ^v	0.982	1.78 (3)	2.68 (3)	149.9 (26)
O11 ^v —HO11 ^v \cdots O23 ^{iv}	0.976	2.74 (4)	3.00 (4)	95.6 (21)
O12 ^v —HO12 ^v \cdots O12 ^v	0.977	2.18 (3)	2.55 (3)	101.3 (18)
O13 ^v —HO13 ^v \cdots O12 ^v	0.985	2.74 (4)	2.86 (4)	87 (3)
O16 ^v —HO16 ^v \cdots O12 ⁱⁱⁱ	0.984	1.82 (4)	2.48 (4)	121.0 (24)
O22—HO22 \cdots O23 ^{vi}	0.986	1.97 (4)	2.83 (4)	144.1 (21)
O23—HO23 \cdots O26 ^{vi}	0.988	2.04 (4)	2.84 (4)	136.6 (21)
O24—HO24 \cdots O15 ^{vii}	0.981	2.15 (3)	3.05 (3)	151.9 (20)
O26—HO26 \cdots O22 ⁱ	0.981	1.86 (3)	2.54 (3)	124.4 (23)
O21 ^{viii} —HO21 ^{viii} \cdots O14 ^{viii}	0.983	2.82 (3)	3.02 (3)	91.7 (19)
O22 ^{viii} —HO22 ^{viii} \cdots O26 ⁱⁱⁱ	0.986	2.35 (3)	3.09 (3)	131.2 (16)
O23 ^{viii} —HO23 ^{viii} \cdots O25	0.979	1.97 (3)	2.81 (3)	142.5 (23)
O26 ^{viii} —HO26 ^{viii} \cdots O22 ^v	0.978	1.91 (3)	2.52 (3)	117.5 (19)

Symmetry codes: (i) $x + 1, y, z + 1$; (ii) $x + 1, y, z$; (iii) $x, y, z + 1$; (iv) $x, y - 1, z - 1$; (v) $x - 1, y, z - 1$; (vi) $x - 1, y, z$; (vii) $x, y + 1, z + 1$; (viii) $x, y, z - 1$; (ix) $x + 1, y, z - 1$; (x) $x + 1, y + 1, z$.

along [100]. This shape is in agreement with the results found with a preferred orientation analysis.

To conclude, the structures of the five crystalline forms of lactose are now known. They were determined from X-ray diffraction with single crystals for two of them (α L-H₂O and β L) and with powder for the three others (α L_H, α L_S and

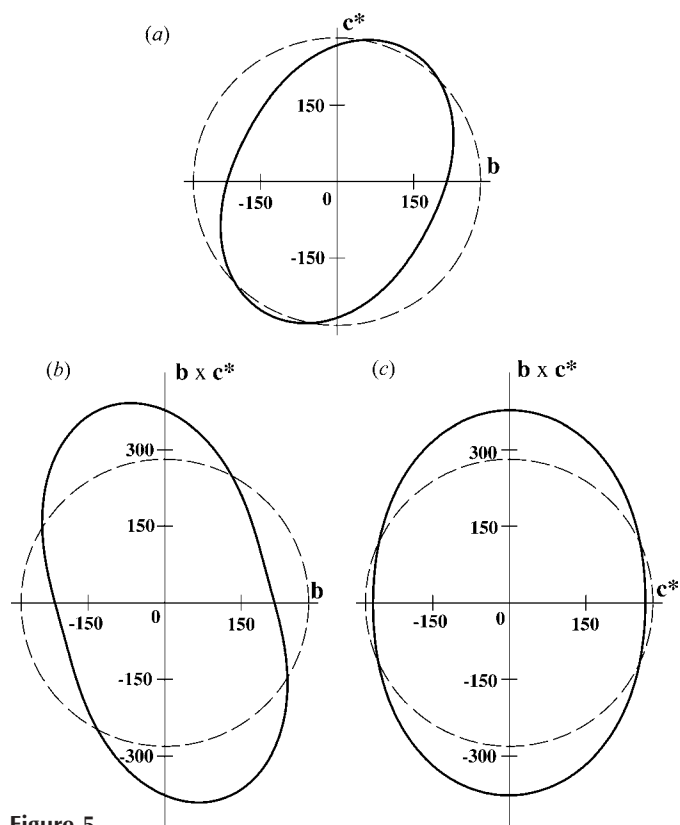


Figure 5
Average shape of the crystallites of mixed 1/1 α/β -lactose: (a) in the bc^* plane; (b) in the bbc^* plane; (c) in the c^*bc^* plane. The dashed circle corresponds to the average diameter of 563 Å.

α/β L). The lattice parameters and the structure of the β L form are completely different to those of the four other forms. The cells of these four forms have almost identical parameters and the long axis of the lactose molecules is along the **b** direction. α L-H₂O and α L_H, on one hand, α L_S and α/β L, on the other, exhibit some similarities, such as the crystalline system, space group and hydrogen-bonding networks. NMR experiments (Fig. 1) show that the chemical shifts measured for the α/β L form, although clearly different, are very similar to those observed for the α L_S polymorph. This suggests, in agreement with X-ray diffraction results, that the structural features of the local molecular environment are qualitatively common to both forms.

References

- Beevers, C. A. & Hansen, H. N. (1971). *Acta Cryst.* **B27**, 1323–1325.
 Bézar, J. F. & Baldinozzi, G. (1993). *J. Appl. Cryst.* **26**, 128–129.
 Brückner, S. & Immirzi, A. (1997). *J. Appl. Cryst.* **30**, 207–208.
 Buma, T. J. & Wiegers, G. A. (1967). *Neth. Milk Dairy J.* **21**, 208–213.
 Caglioti, G., Paoletti, A. & Ricci, F. P. (1958). *Nucl. Instrum.* **3**, 223–228.
 Chu, S. S. C. & Jeffrey, G. A. (1968). *Acta Cryst.* **B24**, 830–838.
 Dincer, T. D., Parkinson, G. M., Rohl, A. L. & Ogden, M. I. (1999). *J. Cryst. Growth*, **205**, 368–374.
 Dollase, W. A. (1986). *J. Appl. Cryst.* **19**, 267–272.
 Drapier-Beche, N. (1997). Thesis, INPL, France.
 Evain, M., Deniard, P., Jouanneaux, A. & Brec, R. (1993). *J. Appl. Cryst.* **26**, 563–569.
 Farrugia, L. (1997). *J. Appl. Cryst.* **30**, 565.
 Favre-Nicolin, V. & Cerny, R. (2002). *J. Appl. Cryst.* **35**, 734–743.
 Fries, D. C., Rao, S. T. & Sundaralingam, M. (1971). *Acta Cryst.* **B27**, 994–1005.
 Garnier, S. (2001). Thesis, University of Rouen, France.
 Ha, S. N., Giammona, A., Field, M. & Brady, J. W. (1988). *Carbohydr. Res.* **180**, 207–221.
 Ham, J. T. & Williams, D. G. (1970). *Acta Cryst.* **B26**, 1373–1383.
 Hirotsu, K. & Shimada, A. (1974). *Bull. Chem. Soc. Jpn.* **47**, 1872–1879.
 Jeffrey, G. A. (1990). *Acta Cryst.* **B46**, 89–103.
 Le Bail, A., Duroy, H. & Fourquet, J. L. (1988). *Mater. Res. Bull.* **23**, 447–452.
 Lerk, C. F., Andreae, A. C., de Boer, A. H., de Hoog, P., Kussendrager, K. & van Leverink, J. (1984a). *J. Pharm. Sci.* **73**, 856–857.
 Lerk, C. F., Andreae, A. C., de Boer, A. H., de Hoog, P., Kussendrager, K. & van Leverink, J. (1984b). *J. Pharm. Sci.* **73**, 857–859.
 Noordik, J. H., Beurskens, P. T., Bennama, P., Visser, R. A. & Gould, R. O. (1984). *Z. Kristallogr.* **168**, 59–65.
 March, A. (1932). *Z. Kristallogr.* **81**, 285–297.
 Platteau, C., Lefebvre, J., Affouard, F. & Derollez, P. (2004). *Acta Cryst.* **B60**, 453–460.
 Platteau, C., Lefebvre, J., Affouard, F., Willart, J. F., Derollez, P. & Mallet, F. (2005). *Acta Cryst.* **B61**, 185–191.
 Popa, N. C. (2000). *J. Appl. Cryst.* **33**, 103–107.
 Rodriguez-Carvajal, J. (2001). *FULLPROF*, Version 1.9c. LLB, CEA/Saclay, France.
 Rodriguez-Carvajal, J. & Roisnel, T. (2004). Proc. of EPDIC 8, edited by Y. Andersson, E. J. Mittemeijer & U. Welzel, pp. 123–126. Zürich: Trans. Tech. Publications.
 Roisnel, T. & Rodriguez-Carvajal, J. (2002a). *Mater. Sci. Forum*, pp. 378–381.

- Roisnel, T. & Rodriguez-Carvajal, J. (2002*b*). *Mater. Sci. Forum*, pp. 118–123.
- Simpson, T. D., Parrish, F. W. & Nelson, N. L. (1982). *J. Dairy Sci.* **47**, 1948–1954.
- Smith, G. S. & Snyder, R. L. (1979). *J. Appl. Cryst.* **12**, 60–65.
- Smith, W. & Forester, T. R. (1996). *J. Mol. Graphics*, **14**, 136–141.
- Sundaralingam, M. (1968). *Biopolymers*, **6**, 189–213.
- Thompson, P., Cox, D. E. & Hastings, J. B. (1987). *J. Appl. Cryst.* **20**, 79–83.
- Werner, P. E., Eriksson, L. & Westdahl, M. (1985). *J. Appl. Cryst.* **18**, 367–370.
- Willart, J. F., Caron, V., Lefort, R., Danède, F., Prévost, D. & Descamps, M. (2004). *Solid State Commun.* **132**, 693–696.
- Wolff, P. M. de (1968). *J. Appl. Cryst.* **1**, 108–113.